ACS APPLIED MATERIALS & INTERFACES

Research Article

www.acsami.org

Preparation of Cell-Embedded Colloidosomes in an Oil-in-Water Emulsion

Yi Gong, Ai Mei Zhu, Qiu Gen Zhang, Mei Ling Ye, Hai Tao Wang, and Qing Lin Liu*

Department of Chemical and Biochemical Engineering, College of Chemistry and Chemical Engineering, Xiamen University, Xiamen 361005, P. R. China.

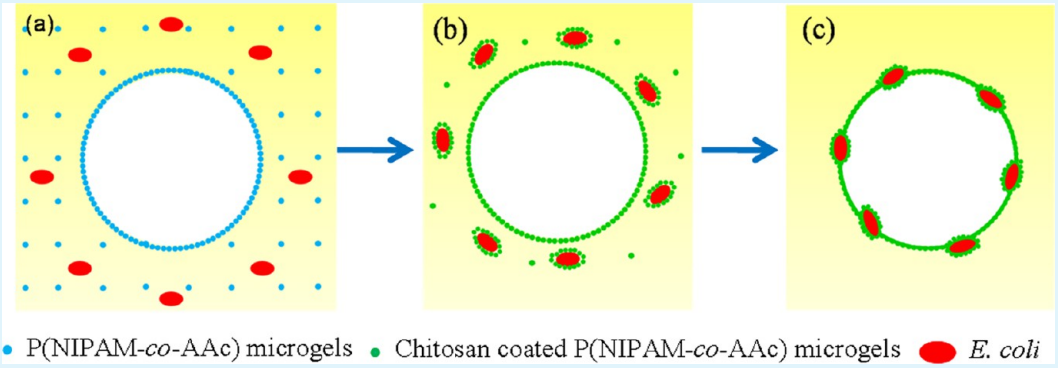

ABSTRACT: Cell encapsulation by locking the interfacial microgels in a water-in-oil Pickering emulsion has currently been attracting intensive attention because of the biofriendly reaction condition. Various kinds of functional microgels can only stabilize an oil-in-water Pickering emulsion, and it is thus difficult to encapsulate cells in the emulsion where the cells are usually dispersed in the continuous phase. Herein, we introduce a facile method for preparing cell-embedded colloidosomes in an oil-in-water emulsion via polyelectrolyte complexation. *Escherichia coli* (*E. coli*) was chosen as a model cell and embedded in the thin shell of chitosan/poly(N-isopropylacrylamide-*co*-acrylic acid) (P(NIPAM-*co*-AAc)) microcapsules. This is beneficial for expressing cell function because of the little resistance of mass exchange between the embedded cells and the external environment. Cells can be used in biocatalysis or biomedicine and our product will hold great promises to improve the performance in those fields. The synthesis route presents a platform to prepare cell-embedded microcapsules in an oil-in-water Pickering emulsion in a facile and biocompatible way. First, an emulsion stabilized by P(NIPAM-*co*-AAc) microgels was prepared. Then, the interfacial microgels in the emulsion were locked by chitosan to form colloidosomes. The mechanism of cell encapsulation in this system was studied via fluorescent labeling. The viability of *E. coli* after encapsulation is ca. 90%. Encapsulated *E. coli* is able to metabolize glucose from solution, and exhibits a slower rate than free *E. coli*. This demonstrates a diffusion constraint through the colloidosome shell.

KEYWORDS: *cell encapsulation, P(NIPAM-co-AAc), microgels, Pickering emulsion, polyelectrolyte complexation, o/w emulsion*

1. INTRODUCTION

Cell encapsulation has currently been attracting intensive attention because of several advantages explored in the literature.[1,2] For example, cells encapsulated in a polymer matrix will be protected from immuno-destruction. Mass exchange between the intercellular and the environment is feasible to maintain the survival and the function of cells because of the permeability of the polymer matrix. This polymer-cell system combines the function of both cells and the polymer and has various potential applications including biomedicine and biocatalysis.[3−5]

Various routes to cell encapsulation have been developed such as cell surface modification,[6] hydrogel encapsulation,[7] and microcapsule (hollow microsphere) encapsulation.[8] Of those, microcapsule is a desirable matrix for cell encapsulation since a larger surface area is provided without modification to cells. Very recently, numerous researchers have focused on this area. For example, Flemke et al.[9] reported preparation and characterization of hollow polymeric microspheres based on the preprecipitation of porous calcium carbonate cores and their use for encapsulation of live *E.coli*. Kim et al.[10] reported encapsulation of *Bacillus thuringiensis* spores using microcapsules via a combination of hydrogels, microfluidic devices, and chemical polymerization. Trongsatitkul et al.[11] fabricated multifunctional core−shell microspheres with biological cells encapsulated within the polymer shell. The cross-linked polymer shell and silicone multicore were formed in situ via photopolymerization within the droplets of an oil-in-water-in-oil double emulsion.

Received: July 12, 2013
Accepted: October 4, 2013
Published: October 4, 2013

Colloidosomes, a kind of microcapsules with shell consisting of packed colloidal particles, have currently been attracting considerable attention.[12−16] Colloidal particles self-assembly on the oil/water interface to stabilize the emulsion droplets are termed a Pickering emulsion.[17] The term of Pickering emulsion broadens by the emergence of a kind of emulsion stabilized by microgels (cross-linked polymer particles swelled by a solvent) which is called a 'Mickering emulsion'.[18] The colloidosomes are usually obtained by locking the interfacial particles in a Pickering emulsion via a feasible technology such as annealing,[19] polyelectrolyte complexation,[20,21] and covalent cross-linking.[22] Colloidosomes have an unique advantage for cell encapsulation involved with preparation and locking of microgels. Encapsulated cells can thus avoid the harsh reaction conditions for the synthesis of microgels since the above two steps are independent. Therefore, the locking process of the interfacial particles in a Pickering emulsion to make a dense shell is crucial for the preparation of colloidosomes. It is feasible that the colloidosomes can be used as a vehicle for cell encapsulation if the locking process is biofriendly. Routh and co-workers[23] reported that the interfacial poly(methylmethacrylate-*co*-butyl acrylate) latex particles in water-in-oil Pickering emulsions were locked together to form colloidosomes with the aid of the diffusion of ethanol. This can be considered as a biofriendly process. Because model cells can be added into a water phase and encapsulated in emulsion droplets, live yeast[15] and lactic acid bacteria[16] are separately encapsulated by colloidosomes successfully in their successive work.

One has to face some challenges for encapsulating cells into colloidosomes. The continuous phase of a Pickering emulsion is normally the one in which the particles are preferentially dispersed.[18] It is known that many functional microgels have excellent hydrophilicity. So a Pickering emulsion that stabilizes those hydrophilic microgels is usually an oil-in-water emulsion. The cells in the aforementioned emulsion are usually dispersed in water (a continuous phase) and thus difficult to be encapsulated.

Herein, we introduce a facile route to prepare cell-embedded colloidosomes in an oil-in-water emulsion. The most studied gram-negative bacterium, *Escherichia coli* (*E. coli*) was chosen as a model cell. As one of the stimuli-responsive materials, P(NIPAM-*co*-AAc) has been widely studied[11,24−26] and designed into different forms to meet various requirements. The emulsion stabilized by P(NIPAM-*co*-AAc)[27] or PNIPAM[28] microgels is carefully studied. P(NIPAM-*co*-AAc) microgels were chosen as a matrix to encapsulate *E. coli* in this work. Polyelectrolyte complexation was used to lock the interfacial microgels in an oil-in-water Pickering emulsion. Since both the microgels and *E. coli* are negatively charged, the positively charged chitosan was used as a complexing agent leading to the formation of *E. coli*-embedded colloidosomes. The resulting composite biomaterials combine the function of both P(NIPAM-*co*-AAc) microgels and *E. coli*. The shell of the colloidosomes where cells are embedded not only protects the embedded cells but also facilitates the mass exchange between the cells and the environment. So our product has all the features possessed by common cell-containing microcapsules. Moreover, a characteristic sets our product apart from others. Since the colloidosome shell is comprised by one or few thin layers of microgels, the resistance of mass exchange between the embedded cells and the external environment will be less than other microspheres[11] or colloidosomes[15,16] with cells in the interior of the vehicle. It will be beneficial for cells to express their function. Cells can be used in biocatalysis or biomedicine. Our product will hold great promises to improve the performance in those fields. Most of all, the proposed route can be realized under mild reaction conditions. This biofriendly synthesis will make significant contributions to cell encapsulation.

2. MATERIALS AND METHODS

2.1. Materials. *E. coli* was kindly donated by Professor Baishan Fang from the Department of Chemical and Biochemical Engineering at Xiamen University (Xiamen, China). N-Isopropylacrylamide (NIPAM) was purchased from Tokyo Chemical Industry Co. Ltd. Chitosan (25 kDa, deacetylation degree 90%) was purchased from Aladdin Reagent (Shanghai) Co., Ltd. N, N-methylenebisacrylamide (MBA, analytical grade) was purchased from the fifth Plant of Shenyang Reagent Co. Ltd. Soybean oil was purchased from the supermarket (Arawana brand refined soybean oil). Acrylic acid (AAc), fluorescein isothiocyanate (FITC), fluorescein isothiocyanate labeled dextran (FITC-Dex, 4.4 kDa) and rhodamine B were purchased from Sigma Aldrich and used as received. LIVE/DEAD BacLight Bacterial Viability Kit (L7007) was purchased from Molecular Probes (Invitrogen). The water used in this work was purified by a Milli-Q reagent grade system. All the other chemicals were supplied from Shanghai Chemical Reagent Store (China) and used without further purification.

2.2. Preparation and Characterization of Pickering Emulsion. P(NIPAM-*co*-AAc) microgels were synthesized via dispersion polymerization. Briefly, 1.2500 g of NIPAM, 125 μL of AAc, 125 mg of MBA, and 20 mg of ammonium persulfate (APS) were dissolved in 100 g of deionized water. The resulting solution was then poured into a flask equipped with a stirrer and a N_2-inlet. Then the whole apparatus was put into a microwave reactor. The polymerization was triggered after bubbling with N_2 for 10 min with the microwave power set to 800 W and a constant temperature of 70 °C. After a specific time, the formed microgels were isolated via centrifugation at 12 000 rpm and then washed using deionized water 3 times. The microgels (3 mL, 20 mg/mL) were characterized by dynamic light scattering (DLS) (Malvern Autosizer 4700) to show the average hydrodynamic diameter of 278 ± 13 nm. The DLS measurements were done at 25 ± 0.1 °C, a fixed scattering angle of 90° and refractive indices set to 1.3. The measurement was repeated 5 times. The microgels were characterized by transmission electron microscopy (TEM) (JEM-2100 JEOL) by placing one drop of the sample on copper grids coated with carbon. Figure 1 shows the TEM image of the P(NIPAM-*co*-AAc) microgels.

Two milliliters of microgels dispersion (20 mg/mL) and 1 mL of *E. coli* suspension (OD_{670} = 1.0000) were mixed together to form a water phase. *E. coli* concentrations were determined by measuring optical

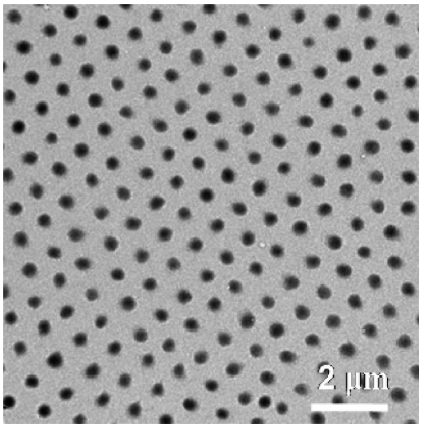

Figure 1. TEM image of the P(NIPAM-*co*-AAc) microgels.

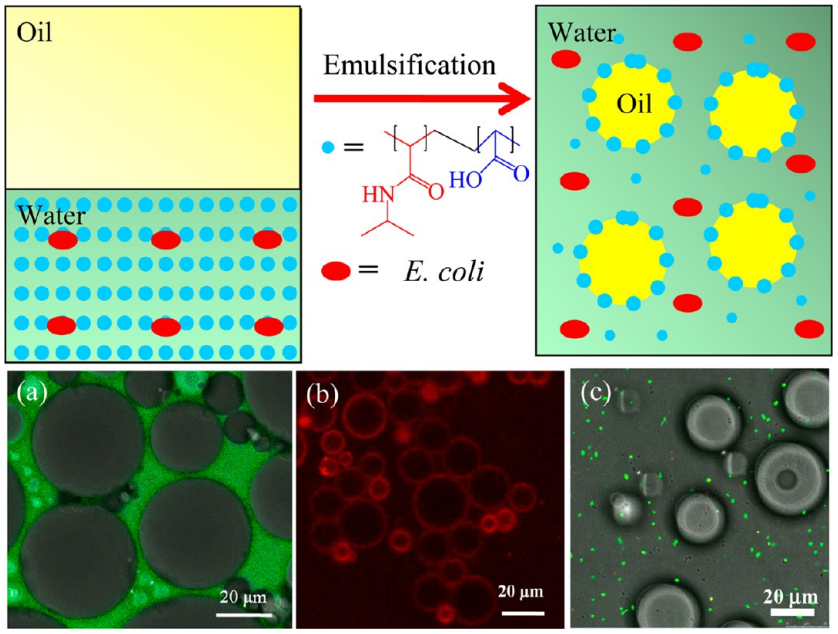

Figure 2. Illustration of the fabrication of a Pickering emulsion. Merged CLSM image of (a) the Pickering emulsion with FITC-Dex dissolved in a water phase, (b) the microgels stained by rhodamine B, and (c) the dispersion of *E. coli* stained by bacterial viability kit in a Pickering emulsion.

density (OD) at 670 nm using a fluorescence spectrophotometer (F-7000, Hitachi, Ltd., Japan). 3.0 g of soybean oil was used as an oil phase. The two phases were then mixed in a microtube (20 mL) and emulsified using a vortex mixer (QL-901, 400W, Haimen City Qilin Medical Instrument Factory, China) for 20 s. The resulting emulsion was thus obtained and characterized by confocal laser scanning microscopy (CLSM). The water phase, the microgels and *E. coli* were stained by FITC-Dex (20 mg/100 mL), rhodamine B (20 mg/100 mL) and Bacterial Viability Kit respectively to study the emulsion type, the microgels and *E. coli* distributions. The samples were prepared by the placing a drop of emulsion between the slides and cover glasses. The sample was excited using both a HeNe 561 nm laser and a 488 argon ion laser together. Emission was detected from 580 to 650 nm for rhodamine B, and from 500 to 545 nm for FITC-Dex and stained cells. This CLSM measurement was repeated 3 times.

2.3. Preparation and Characterization of Cell-Embedded Colloidosomes. Chitosan is labeled using FITC by the method reported in the literature.[29] Briefly, 100 mL of anhydrous methanol and 50 mL of 2.0 mg/mL of FITC in methanol were put into 100 mL of 1% w/v chitosan in 1 wt % acetic acid solution. After reaction in the dark at ambient temperature for 3 h, the FITC labeled chitosan (FITC−CS) was precipitated in 0.2 M NaOH. The products were washed by centrifugation using a water/methanol (v/v = 1:1) mixture until FITC in the supernatant cannot be detected via fluorescence spectrophotometer. The sample was then dried in vacuum for further use.

The as-formed emulsion in a microtube equipped with a magnetic stirrer was stirred at a speed of 400 rpm. One ml of chitosan solution (1% in 1% acetic acid solution) was added dropwise into the emulsion. The reaction was allowed to take place for 10 h. Then the cell-embedded colloidosomes were formed and characterized by CLSM. For easy observation, *E. coli* which can express red fluorescent protein is employed. The samples were prepared as above-mentioned. Similarly, the sample was then excited using both a HeNe 561 nm laser and a 488 argon ion laser together. Emission was detected from 580 to 650 nm for *E. coli*, and from 500 to 545 nm for the FITC−CS. The CLSM observation was repeated 5 times. The average diameter and size distribution of the colloidosomes were measured from the CLSM images.

To wash the colloidosomes, we centrifuged the mixture at 4000 rpm for 10 min. This constrains the colloidosomes to the boundary of the oil and the aqueous phases. Consequently, the cell-embedded colloidosomes were obtained after removing the oil and the aqueous phases using a Pasteur pipet. The resulting colloidosomes were washed using 0.85 wt % NaCl solution for 3 times to test cell viability and activity. After washing by 1 wt % sodium dodecyl benzene sulfonate (SDBS) solution for 7 times during one week to remove the residual oil, the cell-embedded colloidosomes were characterized using scanning electron microscopy (SEM) LEO1530 (Germany). For this, a drop of the sample was put onto a silicon wafer substrate and sputter coated with a homogeneous gold layer for charge dissipation during SEM imaging.

2.4. Tests of Cell Viability and Activity. Fluorescent molecular probes were used to evaluate the *E. coli* cells' viability. Bacterial Viability Kit contains components A and B. Both of them are the mixture of SYTO 9 and propidium iodide. With both metabolically active and plasma membrane integrity, live cells show distinctive green fluorescent intravacuolar structures after being stained by Bacterial Viability Kit. Dead cells, however, exhibit extremely bright red fluorescence. The process for staining the samples involved in adding 3 μL of the mixture of components A and B (1:1) solution into 1 mL of the colloidosomes and *E. coli* sample. The sample was then thoroughly mixed before incubating in the dark at room temperature for 30 min for characterization by CLSM. During CLSM test, the sample was also excited using both a HeNe 561 nm laser and a 488 argon ion laser together. Emission was detected from 620 to 650 nm for dead *E. coli*, and from 510 to 540 nm for live *E. coli*.

The activity of the colloidosome encapsulated *E. coli* was investigated by glucose consumption. The colloidosomes were exposed to 0.26% antiseptic-germicide solution (Guangzhou Blue Moon Industrial Co., Ltd., China) for 10 min to kill all the free *E. coli* and then washed using 0.85 wt % NaCl solution for 3 times. For contrast, 0.5 g (wet weight) of the cell-embedded colloidosomes, 0.5 g (wet weight) of the blank colloidosomes and 1 mL of *E. coli* suspension (OD_{670} = 1.000) were separately added into a 15 mL of 4.6 mM glucose solution to prepare three samples. Then the samples were placed in a shaker (25 °C, 100 rpm). A small volume (10 μL) was extracted from the samples with a pipet at various time intervals and fed to glucose monitoring test strips (ACCU-CHEK Active). Cell viability is calculated as follows

$$V = \frac{N_{green}}{N_{green} + N_{red}}$$

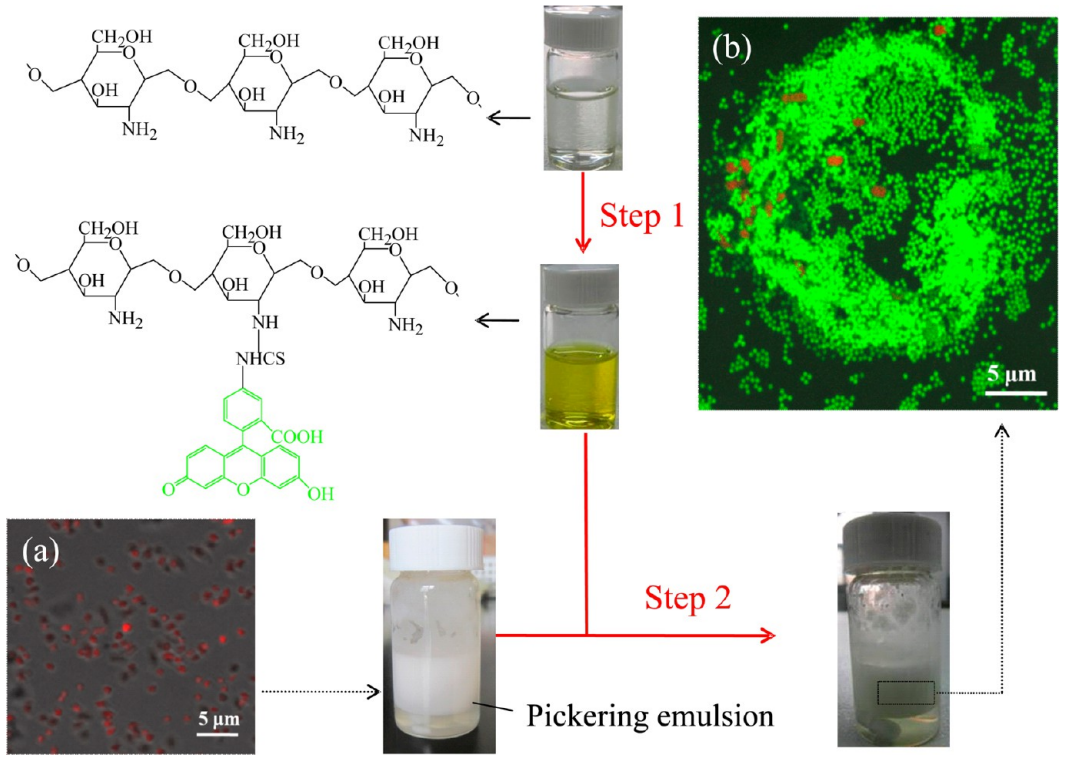

Figure 3. Schematic for preparation of the cell-embedded colloidosomes. Merged CLSM image of (a) *E. coli* and (b) the colloidosomes in the initial stage of formation.

where V is the cell viability, N_{green} is the number of cells in green fluorescence (live cells), and N_{red} is the number of cells in red fluorescence (dead cells).

3. RESULTS AND DISCUSSION

3.1. Preparation of a Pickering Emulsion. Preparation process and the as-prepared Pickering emulsion stabilized by P(NIPAM-*co*-AAc) microgels are illustrated in Figure 2. The P(NIPAM-*co*-AAc) microgels and *E. coli* cells are dispersed in water. The resulting water suspension was emulsificated with oil phase leading to the formation of a Pickering emulsion. To study the type of the Pickering emulsion, we dissolved fluorescein isothiocyanate labeled dextran (FITC-Dex) in water. With green emission (FITC-Dex) outside of the droplets (Figure 2a), the oil-in-water Pickering emulsion can be clearly identified by the merged CLSM image. To verify the distribution of the microgels in the emulsion, we stained the microgels by rhodamine B. As shown in Figure 2b, the emulsion droplets in the shape of red spherical ring were observed by CLSM. This indicates that the interface of the emulsion droplets consists of the stained microgels. The microgels situate on the surface of the emulsion droplets to stabilize the emulsion. *E. coli* cells were stained by the bacterial viability kit to study their distribution in the emulsion. As shown in Figure 2c, cells with green fluorescent are dispersed in the continuous phase outside the emulsion droplets. So the emulsion type, the microgel distribution and cell distribution in the emulsion are characterized and the results are consistent with what one expected (cartoon in Figure 2).

3.2. Preparation of Cell-Embedded Colloidosomes. Because the P(NIPAM-*co*-AAc) microgels are negatively charged, a cationic polyelectrolyte is an ideal material to lock the microgels in the emulsion. As a natural cationic polyelectrolyte with excellent biocompatibility, chitosan is adopted in this work. Fluorescent labeling is used in the synthesis to elucidate the formation of colloidosomes. As shown in step 1 of Figure 3, chitosan is labeled using FITC by the method introduced in the literature.[29] The resulting FITC labeled chitosan (FITC−CS) with a green fluorescent was added into the above-mentioned Pickering emulsion for the synthesis of colloidosomes (step 2 of Figure 3).

The employed *E. coli* can produce red fluorescent protein (as shown in Figure 3a) for labeling. After reaction for 10 min (insufficient reaction time), the emulsion was observed using CLSM. As shown in Figure 3b, the green dots are the P(NIPAM-*co*-AAc) microgels coated by FITC−CS via electrostatic adsorption. Some parts of the microgels are linked together to exhibit a strong green fluorescent. This phenomenon indicates that chitosan can lock the negatively charged microgels via polyelectrolyte complexation. The whole green round shape indicates that the detected area is located in the emulsion droplets. The red rods in Figure 3b are *E. coli* surrounded by the green dots (microgels). This indicates that the negatively charged *E. coli* could also be linked into the interfacial microgels via complexation. Moreover, *E. coli* moved from the continuous phase to the oil−water interface. This behavior is discussed in section 3.3.

To clearly study the structure of the colloidosomes, we employed CLSM to characterize the cell-embedded colloidosomes prepared using fluorescent labeled materials. Figure 4a shows the merged CLSM image of the surface of a colloidosome in the emulsion. The colloidosome shell produces green fluorescent. This suggests that the microgels were locked by chitosan, leading to the shell formation. The red rods (*E .coli*) were immobilized by the colloidosome shell. Figure 4b shows the cross-section of the colloidosome in the emulsion. Fluorescent signal cannot be detected inside of the colloidosome reflecting the microcapsule structure of the

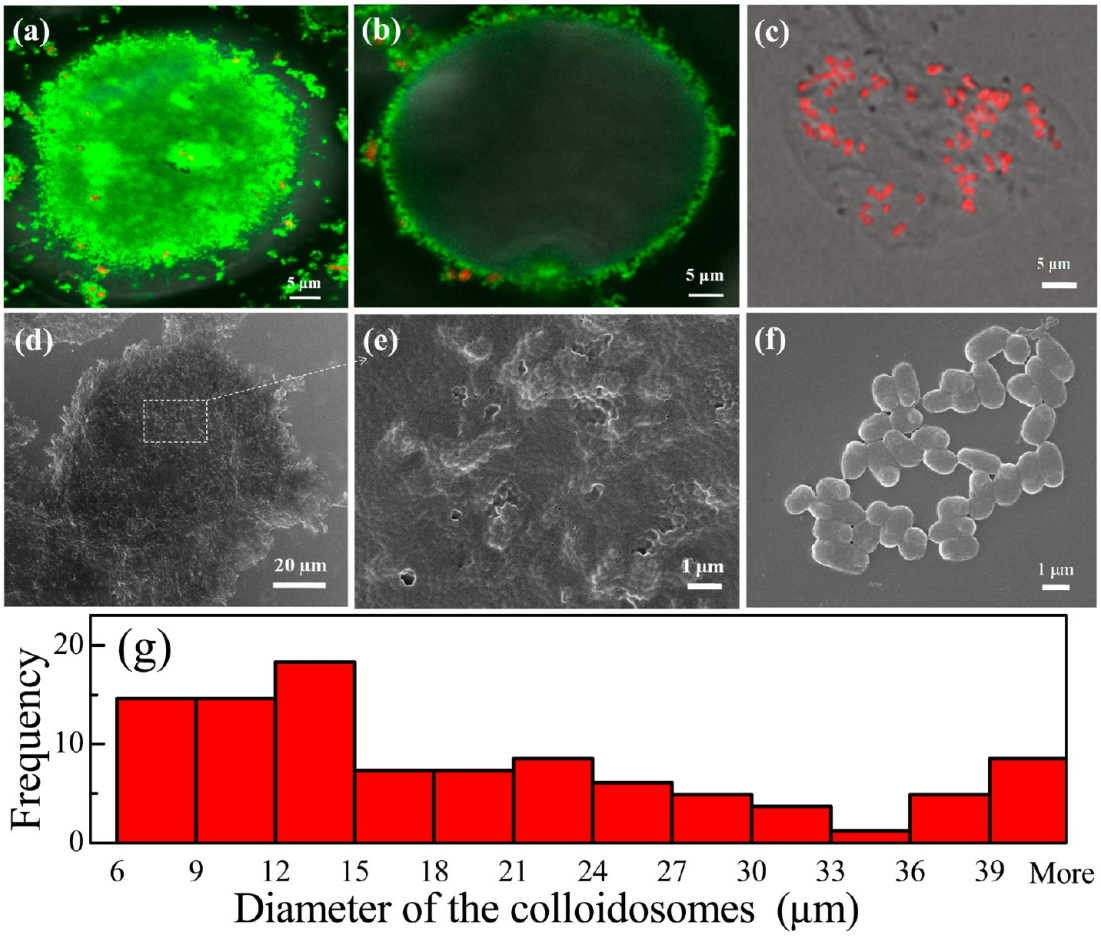

Figure 4. Merged CLSM image of (a) the surface and (b) the cross-section of a cell-embedded colloidosome prepared by FITC−CS. (c) Merged CLSM image of the cell-embedded colloidosome prepared by unlabeled chitosan. (d, e) SEM images of the colloidosome and (f) free *E. coli*. (g) Histogram of the measured size of colloidosomes.

colloidosome. The red rods (*E .coli*) are embedded in the colloidosome shell. This interesting structure would have potential application for catalysis in a biphasic system.[30] Merged CLSM image of the colloidosome prepared by unlabeled chitosan is shown in Figure 4c. *E. coli* cells immobilized onto the colloidosome could be easily distinguished. The cell-embedded colloidosomes were also characterized by SEM. Figure 4d shows a cell-embedded colloidosome which exhibits a fully sphere structure with several nodes on its surface. Figure 4e shows the colloidosome shell comprised of locked microgels. The size of the nodes is consistent with the size of free *E. coli* (Figure 4f). This suggests that the nodes are associated with the embedded *E. coli*. So, one concludes that *E. coli* cells are encapsulated by the colloidosomes. The embedded cells are confirmed to be irreversibly locked in the colloidosomes from SEM characterization of the colloidosomes after washing for 1 week. The size of the colloidosomes was measured from CLSM images. The average diameter (all the microcapsules being approximately taken as spherical) is 21.4 μm, the standard deviation is 16.3 μm, and the measured sizes are shown in a histogram (Figure 4g).

3.3. Formation Mechanism of Cell-Embedded Colloidosomes. It is found that the Pickering emulsion stabilized by the P(NIPAM-*co*-AAc) microgels is an oil-in-water emulsion and *E. coli* cells are dispersed in the continuous phase. It is important to understand how this system can lead to cell encapsulation. The formation mechanism of the cell-embedded colloidosomes is studied in this work. Two steps (Figure 5) are proposed in the formation of cell encapsulation: adsorption (step A) and locking (step B) of chitosan. The original state of the Pickering emulsion without adding chitosan solution was characterized (Figure 2), as shown in Figure 5a. The P(NIPAM-*co*-AAc) microgels are dispersed in the continuous phase and the surface of the emulsion droplets while *E. coli* cells are dispersed only in the continuous phase. When the chitosan solution was added into the emulsion (step A of Figure 5), the chitosan molecules diffused in the continuous phase. Because the chitosan is positively charged, whereas the microgels and *E. coli* are negatively charged, the chitosan molecules should connect both the microgels and *E. coli* cells to form a microgel−cell complex, as shown in Figure 5b. This phenomenon is confirmed in the water phase. The microgel−cell structure was characterized using CLSM and SEM. Figure 5b1 shows that the chitosan coated microgels (the green dots) are adsorbed on the surface of *E. coli* (the red rods). The same result from SEM (Figure 5b2) shows that a microgel-cell structure is formed. At the same time, the chitosan also diffused into the oil−water interface where numerous microgels located. Chitosan is then coated onto the surface of the microgels. To verify this hypothesis, 0.25 mL of the FITC−CS was added into the Pickering emulsion. Since the amount of chitosan is insufficient, therefore the reaction stays in step A. After reaction for 10 h, the sample was characterized using CLSM. As shown in Figure

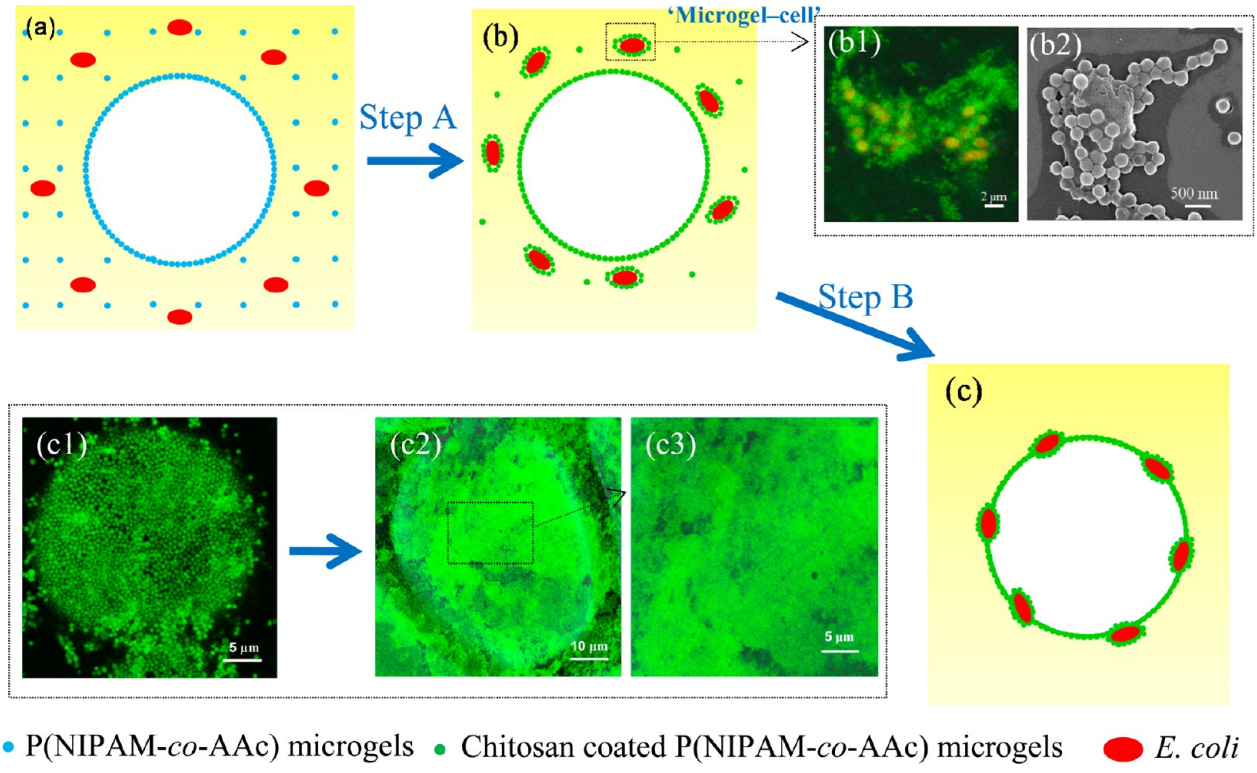

Figure 5. (a–c) Illustration of three stages in the formation of the colloidosomes. (b1) Merged CLSM image and (b2) SEM image of the microgel-cell structure. Merged CLSM image of the Pickering emulsion in which (c1) 0.25 mL and (c2, c3) 1 mL of FITC–CS were added.

5c1, the green dots scattered onto the surface of the emulsion droplet indicate that the microgels are only coated by FITC–CS without forming a shell. We cannot obtain colloidosomes after centrifugation in this situation. This supports the formation mechanism.

During step A, both the surfaces of the microgel–cell and the microgels are immediately chitosan coated via adsorption with the addition of chitosan solution. However, both the adsorptions are not full in an insufficient adsorption time. Therefore, the surfaces tend to adsorb chitosan further. As a result, an adsorption between the microgel–cell and the interfacial microgels can be realized since both their surfaces are chitosan coated. The microgel–cell would then be immobilized on the surface with stirring (as shown in Figure 3b) to start step B. With increasing chitosan diffusion to the surface of the emulsion droplets, the interfacial microgels and the microgel–cell are locked together to form a shell. Consequently, the colloidosomes are formed and *E. coli* cells are embedded in the shell of the colloidosomes (Figure 5c). To verify this process, we studied the effect of the amount of chitosan. When 0.25 mL of FTIC–CS was used, as shown in Figure 5c1, the microgels were coated by FTIC–CS and separated. When 1.00 mL of FTIC–CS was used, the boundary of the microgels cannot be observed (Figure 5c2 and Figure 5c3) and the colloidosomes can be obtained after centrifugation for this case. This suggests the shell of the colloidosomes being formed by increasing the diffusion of chitosan.

3.4. Viability and Activity of *E. coli* after Encapsulation. Cell viability is an important index to evaluate the biocompatibility of cell encapsulation and tested by CLSM in this work. Survival and dead cells present green and red fluorescents respectively; they could be clearly distinguished after being stained by Bacterial Viability Kits. Figure 6 shows

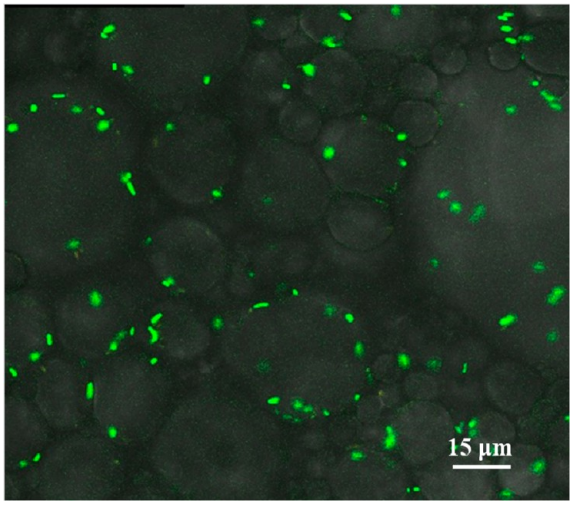

Figure 6. Merged CLSM image of the *E. coli*-embedded colloidosomes. *E. coli* cells were stained by bacterial viability kit.

the stained cells after encapsulation. The cells with green fluorescent suggest a good biocompatibility of the encapsulation process. Most of them are located on the surface of the colloidosomes. Some free *E. coli* can also be observed. Statistics from the CLSM images show that cell viability after encapsulation is ca. 90%. The standard deviation of cell viability is 0.085. This suggests that this encapsulation process is biofriendly.

Chitosan has been used as an antimicrobial agent and can inhibit the growth of a wide variety of bacteria.[31] Figure 6 shows that chitosan cannot kill *E. coli* in this work. This is possibly caused by two reasons. First, the microgels adsorb a certain amount of chitosan resulting in a depression in the

effect of chitosan against *E. coli*. Second, the time for completion of cell encapsulation is 10 h. This may be too short to kill *E. coli*. It is important that chitosan shows its antibacterial activity only in an acidic medium because of its poor solubility above pH of 6.5.[32] The antibacterial activity of chitosan can thus be ignored when the formed colloidosomes are used in a nonacidic medium. Cell viability of 90% suggests the strong adaptability of this method considering the polymer with antimicrobial activity being used in this work.

Cell activity after encapsulation was studied by measuring the glucose consumption. Figure 7 shows the glucose consumption

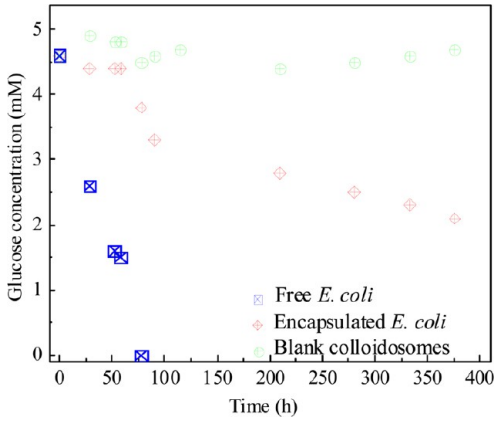

Figure 7. Glucose consumption of different samples. Half a gram (wet weight) of the cell-embedded colloidosomes, 0.5 g (wet weight) of the blank colloidosomes and 1 mL of *E. coli* suspension (OD_{670} = 1.0000) were separately added into 15 mL of 4.6 mM glucose solution. The glucose concentration of the samples was measured at various times.

trend by colloidosome-encapsulated *E. coli*. For comparison, glucose concentration was also measured for free *E. coli* to investigate the effect of encapsulation on the rate of glucose consumption. There are two main differences in the trend between encapsulated *E. coli* and free *E. coli*. First, the glucose concentration has only a slight decrease in the first 60 h for encapsulated *E. coli*. This may be due to the slow diffusion of glucose through the colloidosome shell. Therefore, there must be a considerable glucose molecules diffusion resistance through the colloidosome shell. Second, the rate of glucose consumption by encapsulated *E. coli* is much slower. This may be caused by the slow diffusion of glucose and below 100% encapsulation efficiency. On the other hand, these phenomena confirm that *E. coli* cells were successfully encapsulated in the colloidosomes. For comparison, the same measurements were recorded for the blank colloidosomes (without *E. coli*). No obvious decrease in glucose concentration can be observed over time for the blank colloidosome samples. This verifies that the glucose consumption observed in the sample of encapsulated *E. coli* is only due to the encapsulation.

4. CONCLUSIONS

In summary, a novel method for preparing cell-embedded colloidosomes in an oil-in-water emulsion has been demonstrated. Fluorescent labeling technology was employed to study the formation mechanism. The microgels and *E. coli* are linked together to form a microgel−cell structure taking full advantage of the electrostatic adsorption between the microgels (*E. coli*) and chitosan. The microgel−cell complexes are immobilized onto the surface of emulsion droplets full of the microgels under stirring because of the electrostatic adsorption. Then the chitosan in the water phase continuously diffuses onto the surface of the emulsion droplets leading to the formation the colloidosomes. *E. coli* cells are embedded in the thin shell of the colloidosomes. Cell viability after encapsulation is ca. 90%. This suggests this route is biofriendly. Encapsulated *E. coli* is able to metabolize glucose from solution, and exhibits a slower rate than free *E. coli*. Because of the flexibility in choosing functional microgels and cells, this approach reveals interests in preparation of cell-embedded colloidosomes in an oil-in-water emulsion. Because mild reaction condition and nontoxic reagent are used, the facile methodology present in the study provides a green and facile way to cell encapsulation.

AUTHOR INFORMATION

Corresponding Author

*E-mail: qlliu@xmu.edu.cn. Tel: 86-592-2188072. Fax: 86-592-2184822.

Notes

The authors declare no competing financial interest.

ACKNOWLEDGMENTS

Financial support from National Nature Science Foundation of China Grants 21376194 and 21076170, and the research fund for the Priority Areas of Development in Doctoral Program of Higher Education (20130121130006) in preparation of this article are gratefully acknowledged. We are greatly thankful for the referees' constructive comments.

REFERENCES

(1) Bhatia, S. R.; Khattak, S. F.; Roberts, S. C. *Curr. Opin. Colloid Interface Sci.* **2005**, *10*, 45−51.
(2) Orive, G.; Hernández, R. M.; Gascón, A. R.; Calafiore, R.; Chang, T. M.; De Vos, P.; Hortelano, G. *Nat. Med.* **2003**, *9*, 104−107.
(3) Kong, H. J.; Smith, M. K.; Mooney, D. J. *Biomaterials* **2003**, *24*, 4023−4029.
(4) Zielinski, B. A.; Aebischer, P. *Biomaterials* **1994**, *15*, 1049−1056.
(5) Chia, S. M.; Wan, A. C.; Quek, C. H.; Mao, H. Q.; Xu, X.; Shen, L.; Ng, M. L.; Leong, K. W.; Yu, H. *Biomaterials* **2002**, *23*, 849−856.
(6) Teramura, Y.; Iwata, H. *Soft Matter* **2010**, *6*, 1081−1091.
(7) Schmidt, J. J.; Rowley, J.; Kong, H. J. *J. Biomed. Mater. Res. A* **2008**, *87*, 1113−1122.
(8) Rabanel, J. M.; Banquy, X.; Zouaoui, H.; Mokhtar, M.; Hildgen, P. *Biotechnol. Prog.* **2009**, *25*, 946−963.
(9) Flemke, J.; Maywald, M.; Sieber, V. *Biomacromolecules* **2012**, *14*, 207−214.
(10) Kim, B. I.; Jeong, S. W.; Lee, K. G.; Park, T. J.; Park, J. Y.; Song, J. J.; Lee, S. J.; Lee, C. S. *Sensors* **2012**, *12*, 10136−10147.
(11) Trongsatitkul, T.; Budhlall, B. M. *Langmuir* **2011**, *27*, 13468−13480.
(12) Shilpi, S.; Jain, A.; Gupta, Y.; Jain, S. K. *Crit. Rev. Ther. Drug Carrier Syst.* **2007**, *24*, 361−391.
(13) San Miguel, A.; Behrens, S. H. *Soft Matter* **2011**, *7*, 1948−1956.
(14) Eze, N. A.; Milam, V. T. *Soft Matter* **2013**, *9*, 2403−2411.
(15) Keen, P. H.; Slater, N. K.; Routh, A. F. *Langmuir* **2011**, *27*, 1169−1174.
(16) Keen, P. H.; Slater, N. K.; Routh, A. F. *Langmuir* **2012**, *28*, 16007−16014.
(17) Lee, D.; Weitz, D. A. *Adv. Mater.* **2008**, *20*, 3498−3503.
(18) Richtering, W. *Langmuir* **2012**, *28*, 17218−17229.
(19) Dinsmore, A.; Hsu, M. F.; Nikolaides, M.; Marquez, M.; Bausch, A.; Weitz, D. *Science* **2002**, *298*, 1006−1009.
(20) Gordon, V. D.; Chen, X.; Hutchinson, J. W.; Bausch, A. R.; Marquez, M.; Weitz, D. A. *J. Am. Chem. Soc.* **2004**, *126*, 14117−14122.
(21) Ao, Z.; Yang, Z.; Wang, J.; Zhang, G.; Ngai, T. *Langmuir* **2009**, *25*, 2572−2574.

(22) Shah, R. K.; Kim, J. W.; Weitz, D. A. *Langmuir* **2010**, *26*, 1561−1565.
(23) Nomura, T.; Routh, A. F. *Langmuir* **2010**, *26*, 18676−18680.
(24) Dong, Y.; Ma, Y.; Zhai, T.; Shen, F.; Zeng, Y.; Fu, H.; Yao, J. N. *Macromol. Rapid Commun.* **2007**, *28*, 2339−2345.
(25) Zhang, F.; Wang, C. C. *Langmuir* **2009**, *25*, 8255−8262.
(26) Mohsen, R.; Vine, G. J.; Majcen, N.; Alexander, B. D.; Snowden, M. J. *Colloid. Surf. A* **2013**, *428*, 53−59.
(27) Ngai, T.; Behrens, S. H.; Auweter, H. *Chem. Commun.* **2005**, 331−333.
(28) Tsuji, S.; Kawaguchi, H. *Langmuir* **2008**, *24*, 3300−3305.
(29) Onishi, H.; Machida, Y. *Biomaterials* **1999**, *20*, 175−182.
(30) Wang, Z.; van Oers, M.; Rutjes, F. P.; van Hest, J. *Angew. Chem., Int. Ed.* **2012**, *51*, 10746−10750.
(31) Rabea, E. I.; Badawy, M. E. T.; Stevens, C. V.; Smagghe, G.; Steurbaut, W. *Biomacromolecules* **2003**, *4*, 1457−1465.
(32) Li, Z.; Zhuang, X. P.; Liu, X. F.; Guan, Y. L.; Yao, K. D. *Polymer* **2002**, *43*, 1541−1547.